MULTIVIBRATORS

A multivibrator is a device which transitions (vibrates) between several (multi) fixed output levels. Besides their use for timing, they are commonly used either for storage or for clocking of data in digital computers using binary numbers where the number of levels is generally two. There are several types of multivibrators and several classification schemes. One classification is (1) triggered or (2) free-running. Another more frequent classification method uses their stability properties for which, in the two-level case, there are (1) monostable, (2) bistable, or (3) astable multivibrators. The bistable multivibrator has an output that remains in either of its two stable states until a trigger occurs, which forces a transition to the other stable state; consequently, the name *flip-flop* is frequently ascribed to it. The monostable multivibrator remains in its one stable state until triggered into its unstable state, from which it eventually returns, usually after a fixed transition time, to the stable state; an alternate name of *one-shot* is frequently used for it. The astable multivibrator acts as a nonlinear oscillator as it oscillates periodically between its two unstable states, often in an asymmetrical manner and giving different resting times for each state. Most standard electronic circuits texts contain some material on multivibrators, as, for example, Refs. 1 and 2 as well as Refs. 3 to 6.

GENERIC—BINARY HYSTERESIS MULTIVIBRATOR

A generic form of binary multivibrator is obtained by combining a nonlinearity that is binary hysteresis with a linear load line, a single capacitor for dynamics, and a possible trigger input; the type of multivibrator depends upon the position of the load line on the hysteresis curve. Such a circuit is illustrated in Fig. 1(a), where all signals are taken as voltages referenced to ground; the hysteresis is illustrated in Fig. 1(b). A circuit for the hysteresis is given in Fig. 5, but here we assume infinite input impedance and zero output impedance. If at time t we take $u(t)$ to be the multivibrator (trigger) input, $y(t)$ its output, and $x(t)$ its internal state signal, which is input to the hysteresis $h(x)$, we can write

$$C\frac{dx}{dt} = g_i(u-x) + g_f(y-x) \tag{1}$$

$$y = h(x) \tag{2}$$

in which the constants are the capacitance C, input conductance $g_i = 1/r_i$, and feedback conductance $g_f = 1/r_f$. The binary hysteresis is characterized by

$$y = h(x) = \begin{cases} Y_{lo} & \text{if } X_{lo} \le x \\ Y_{hi} & \text{if } x \le X_{hi} \end{cases} \tag{3}$$

where the constants X_{lo} and X_{hi} are the low and high transition points of the hysteresis, satisfying $X_{lo} < X_{hi}$; Y_{lo} and Y_{hi} are the two output values of the binary hysteresis. The x-axis mid-point of the hysteresis is given by

$$X_{mid} = X_{lo} + \frac{X_{hi} - X_{lo}}{2} = \frac{X_{lo} + X_{hi}}{2} \tag{4}$$

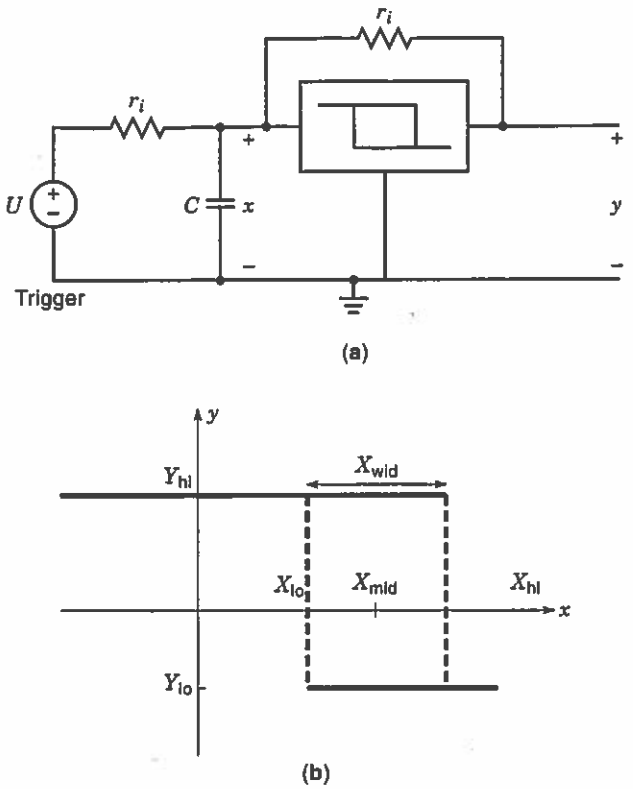

Figure 1. (a) Generic multivibrator using hysteresis. (b) Binary hysteresis. Gives philosophy for all multivibrator types. Hysteresis generated as per Fig. 7(a).

and is seen to represent an offset of the hysteresis curve along the x axis. Of similar importance is the hysteresis width given by

$$X_{wid} = X_{hi} - X_{lo} \tag{5}$$

By considering Eq. (1) at DC we obtain the (untriggered, that is, with $u = 0$) load line for the hysteresis as given by

$$y = \left(1 + \frac{g_i}{g_f}\right)x = Lx \tag{6}$$

which defines the slope $L = [1 + (g_i/g_f)]$, with $L > 1$. Depending upon this slope L the hysteresis mid-point and the hysteresis width, we have three basic types of intersections of the load line with the hysteresis as discussed in the next sections and shown in Fig. 2(a–c).

Monostable Multivibrator

The monostable multivibrator results from the situation shown in Fig. 2(a), where in the absence of an input trigger (that is, $u = 0$), there is one intersection, at the Q point,

$$X_Q = \frac{Y_{hi}}{L} \tag{7}$$

which is stable. In this case the system remains at the intersection point Y_{hi} until there is an input trigger: thus the monostable output Y_{hi}. If a positive input trigger impulse is ap-

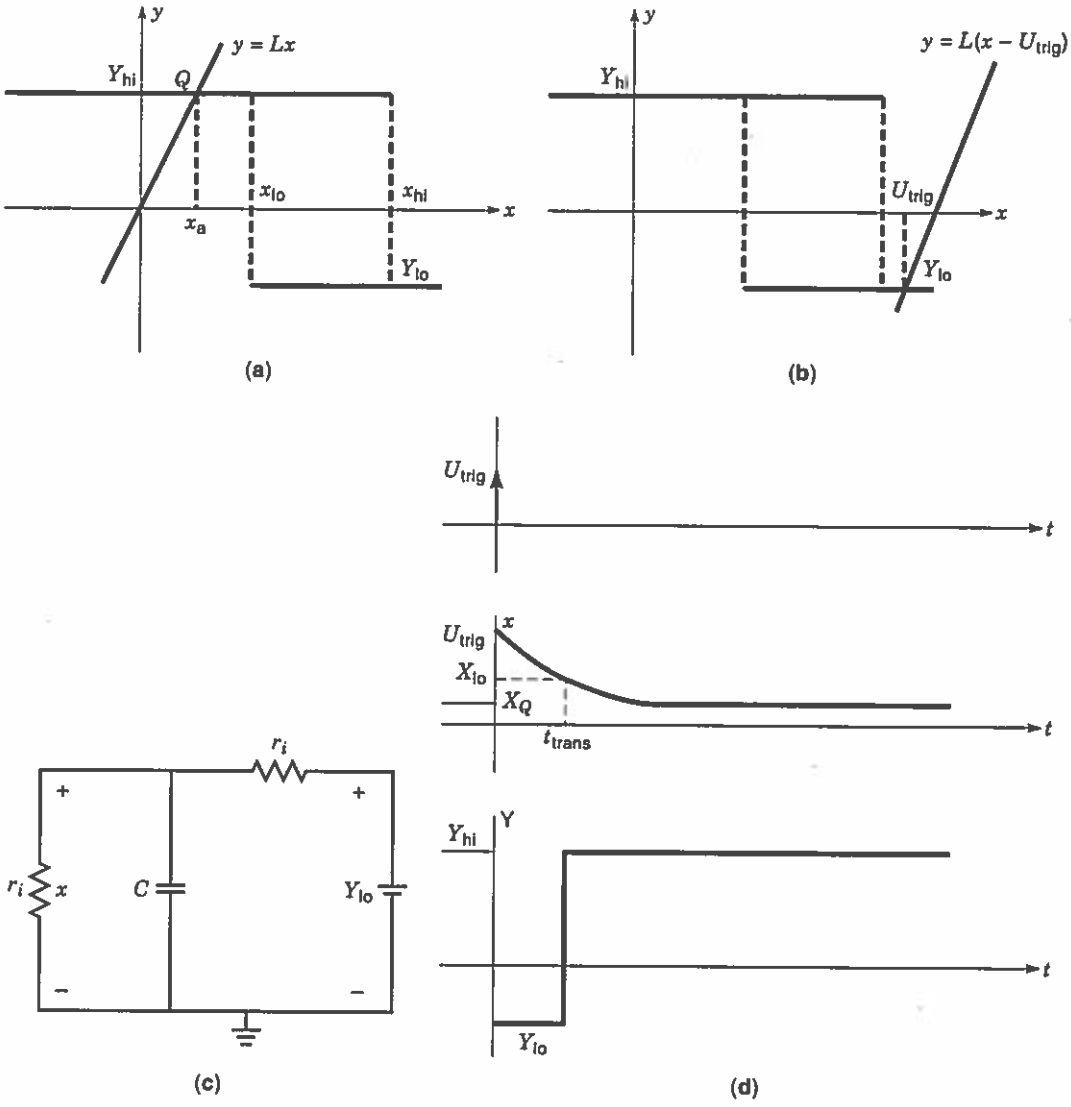

Figure 2. (a) Monostable Q point. (b) Triggered effective load line. (c) Equivalent circuit for transient, $X_{\text{initial}} = U_{\text{trig}} \geq X_{\text{hi}}$. (d) Triggered response. Shows operation of the monostable multivibrator.

plied of peak value U_{trig} [$u(t) = U_{\text{trig}}\delta(t)$ with $\delta(\cdot)$ the unit impulse], which is larger than needed to move the capacitor voltage x past the value X_{hi} ($U_{\text{trig}} \geq X_{\text{hi}}$) then, as shown in Fig. 2(b), this effectively moves the load line to intersect the x axis of the hysteresis at the capacitor initial value (which is the peak trigger voltage value U_{trig}). On removal of the trigger peak, a transient transition is made from the output Y_{lo} back to Y_{hi}. The (minimum) value of this input trigger is seen to be just X_{hi}. The transient return is governed by a time constant determined by C and the Thevenin's equivalent resistor seen by C, that is, with time constant

$$t_{\text{cnst}} = \frac{C}{g_{\text{i}} + g_{\text{f}}} \tag{8}$$

The transition time will be the time to go from the maximum value of x, as determined by the trigger, to X_{lo} with this time constant. An equivalent circuit for determination of this transition time is shown in Fig. 2(c), in which it is seen that x heads toward the low asymptotic value

$$X_{\text{asym-lo}} = Y_{\text{lo}} \frac{g_{\text{f}}}{g_{\text{i}} + g_{\text{f}}} \tag{9}$$

as determined from the voltage division of Y_{lo} between r_{f} and r_{i}. Consequently, assuming that the trigger impulse is applied at $t = 0$, the state for this transition is given as a first order response by

$$x(t) = X_{\text{asym-lo}} + [U_{\text{trig}} - X_{\text{asym-lo}}] \exp\left(-\frac{t}{t_{\text{cnst}}}\right) \tag{10}$$

From Eq. (10) the transition time is found, by setting $x(t_{\text{trans}}) = X_{\text{lo}}$, to be

$$t_{\text{trans}} = -t_{\text{cnst}} \times \ln\left(\frac{X_{\text{lo}} - X_{\text{asym-lo}}}{U_{\text{trig}} - X_{\text{asym-lo}}}\right) \tag{11}$$

where we naturally assume that the asymptotic value is smaller than the jump point value, $X_{asym-lo} < X_{lo}$, so that the transition point X_{lo} can actually be reached. The output y at this transition time jumps back to Y_{hi}. A typical response of this monostable multivibrator to an impulse trigger is shown in Fig. 2(d).

In this case, as illustrated by Fig. 2(a), the output remains at the high level Y_{hi} until a positive input trigger occurs, at which time the output immediately falls to the low level Y_{lo}, where it remains until the signal of the state x falls below X_{lo} as determined by the time constant. A similar situation clearly holds if the load line intersects just the lower branch of the hysteresis curve; but here the transition occurs with a negative impulse input trigger rather than a positive one, and the asymptotic value heads toward the positive value of

$$X_{asym-hi} = Y_{hi}\frac{g_f}{g_i + g_f} \tag{12}$$

Equation (11) remains valid when this asymptotic value is used. In either case, since only one output pulse occurs per input trigger, the monostable multivibrator is often called a one-shot.

Bistable Multivibrator

In the case where the load line intersects both the upper and lower branches of the hysteresis, as shown in Fig. 3, then a bistable multivibrator results, since both intersection points serve as stable rest points. As in the monostable case, an impulse trigger input of sufficiently large amplitude to shift the load line off of one of the hysteresis branches will transition the system to the other stable point. The time constant will again be $C/(g_i + g_f)$, and the system will remain in the state to which it transitioned until another appropriate input trigger makes it transition again. The equations governing the transitions are essentially those developed for the monostable multivibrator with substitutions of the appropriate levels.

Astable Multivibrator

Figure 4 illustrates the astable situation in which the load line intersects the jump lines of the hysteresis. As these intersections are unstable, the system will not rest at either "intersection" but will transition between them with no input required to cause the transition. Again the transitions are

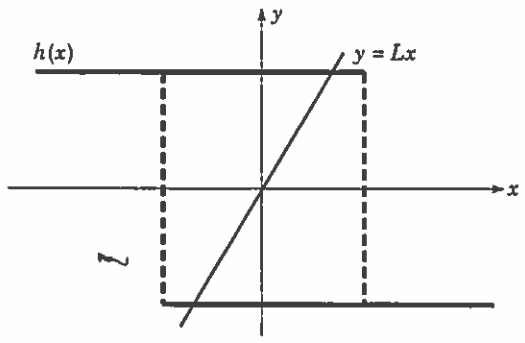

Figure 3. Load line on hysteresis for bistable multivibrator operation.

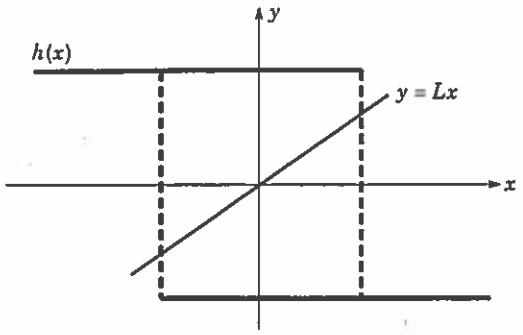

Figure 4. Load line on hysteresis for astable multivibrator operation.

governed by the time constant $C/(g_i + g_f)$, which generally leads to symmetrical output pulses.

To obtain equations for the transition times and the period, we begin by assuming that the multivibrator has just switched from one to the other of its two output levels, taken here for convenience to be from Y_{hi} to Y_{lo}. At that time, normalized to $t = 0$, we again have the equivalent circuit of Fig. 2(c), except that now the initial condition on C is given by x at the switching point, this being X_{hi}. Consequently, the capacitor value heads toward a low value with the mentioned time constant, stopping when x reaches X_{lo}, at which time another transition (from low to high) is initiated. Substitution of the correct initial condition and asymptotic value in Eq. (11) gives the time for transition from the high to the low output, t_{hi-lo}, as

$$t_{hi-lo} = -t_{cnst} \times \ln\left(\frac{X_{lo} - X_{asym-lo}}{X_{hi} - X_{asym-lo}}\right) \tag{13}$$

By changing hi to lo and vice versa, this formula serves to give the transition time from lo to hi as

$$t_{lo-hi} = -t_{cost} \times \ln\left(\frac{X_{hi} - X_{asym-hi}}{X_{lo} - X_{asym-hi}}\right) \tag{14}$$

Consequently the period of oscillation of this astable multivibrator is given by

$$t_{per} = t_{lo=hi} + t_{hi-lo} \tag{15}$$

Note that in the symmetric case where $X_{lo} = -X_{hi}$ and $Y_{lo} = -Y_{hi}$ we have $t_{lo-hi} = t_{hi-lo}$, in which case the period is given by

$$t_{per-sym} = -2\frac{C}{g_i + g_f} \times \ln\left(\frac{-X_{hi} + Y_{hi}\dfrac{g_f}{g_i + g_f}}{X_{hi} + Y_{hi}\dfrac{g_f}{g_i + g_f}}\right) \tag{16}$$

Should asymmetrical output pulses be desired, then a different time constant can be obtained for the rise as compared to the fall by replacing r_i or r_f by a parallel combination of two resistors in series with inverted diodes, as shown in Fig. 5(a–

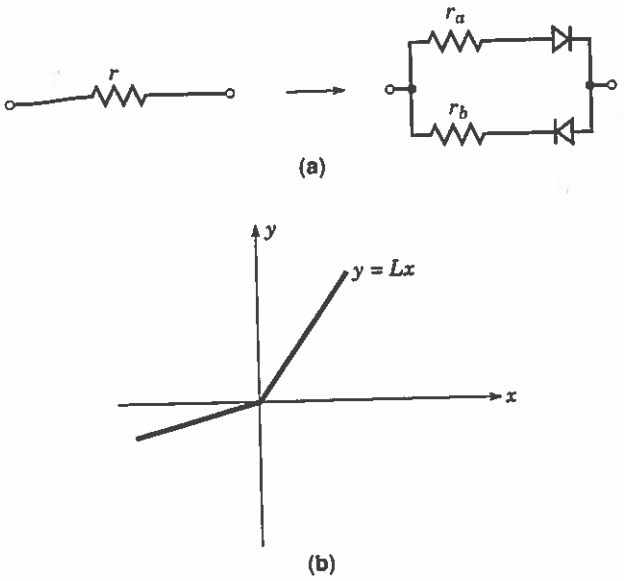

Figure 5. (a) Replacement of r_i or r_f for asymmetrical output. (b) Piecewise linear load line using r_i or r_f replacement. Resistor diode circuit for generation of nonsymmetrical outputs.

b). In fact one of the diodes can be omitted, depending upon which of the two slopes is the biggest. An alternate means of obtaining asymmetry is via hysteresis asymmetry, which will show up inside the logarithmic terms of Eqs. (13) and (14).

Trigger Generation

Since an impulse trigger is desired for triggering the monostable and bistable multivibrators, the standard way to obtain it is by differentiation of a step pulse. Figure 6 shows a typical means of generating a trigger impulse from a step pulse of amplitude V_p. Here the terminals a and b are those of the trigger input u in Fig. 1(a). However, one could alternatively apply the terminals a and b through a diode directly to the multivibrator capacitor (and replace u by a short) to better insure the direct application of desired initial values. This method is most useful in the monostable case, while in the bistable case one would need to switch between two differently directed diodes.

Hysteresis Generation

Figure 7(a) shows an op-amp circuit that generates the binary hysteresis—in essence this is a Schmitt trigger. In Fig. 7(b) we illustrate the means of calculating the hysteresis with the

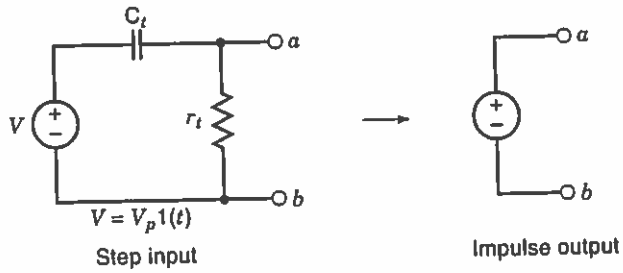

Figure 6. Differentiation circuit for impulse trigger.

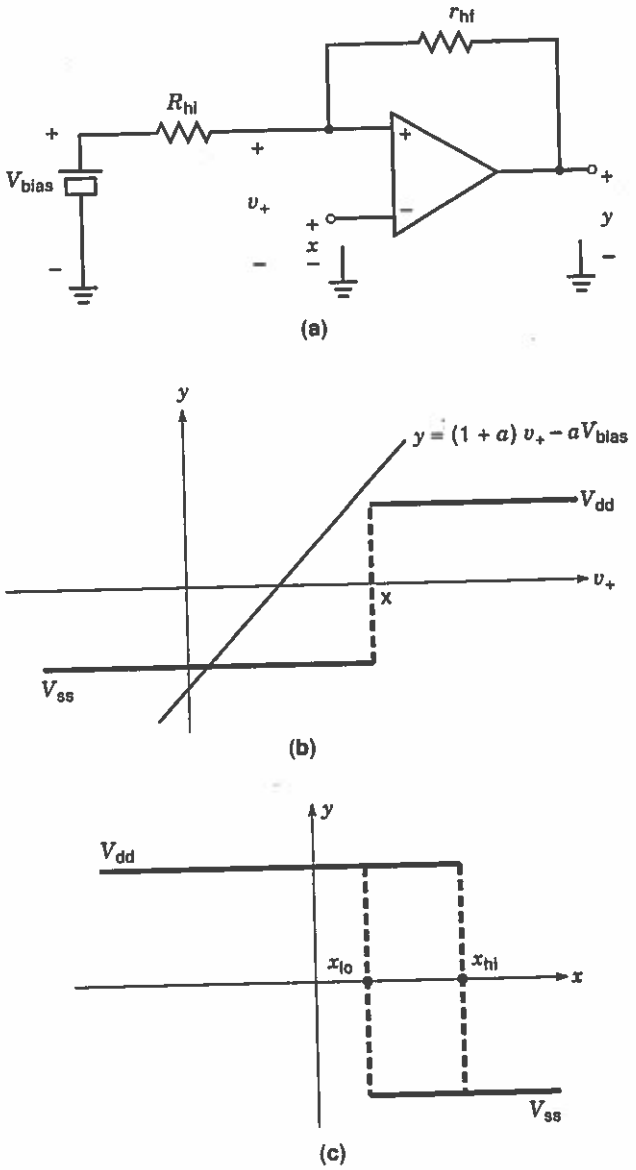

Figure 7. (a) Hysteresis generation circuit using an op-amp. (b) Loading for the generic multivibrator. The op-amp characteristic moves with x to intersect the fixed load line. (c) Resulting hysteresis.

hysteresis curve shown in Fig. 7(c). For Fig. 7(b) we describe the op-amp as a function of v_+, the positive op-amp input terminal voltage with respect to ground, with x as a parameter by

$$y(v_+) = V_{dd} \times 1(v_+ - x) + V_{ss} \times 1(x - v_+) \tag{17}$$

where $1(\cdot)$ is the unit step function and V_{dd} and V_{ss} are the upper and lower power supply voltages. The resistor portion of Fig. 7 acts as a load line on the op-amp characteristic and is described by

$$y(v_+) = (1 + a)v_+ - aV_{bias} \tag{18}$$

$$a = \frac{g_{hi}}{g_{hf}} \tag{19}$$

As seen in Fig. 7(b), when we increase x the op-amp jump moves to the right and eventually the intersection of the two curves remains at V_{ss}, while as we decrease x the op-amp jump moves to the left and eventually the intersection is at V_{dd}. For intermediate values of x there are two intersections. The second one starts, as seen by moving the op-amp curve left, at $v_+ = x$, where $y = V_{dd}$ for both curves. This gives the geometry of Fig. 7(b)

$$X_{hi} = \frac{V_{dd} + aV_{bias}}{1+a} \tag{20}$$

and the value for moving right starts at

$$X_{lo} = \frac{V_{ss} + aV_{bias}}{1+a} \tag{21}$$

These two values give the hysteresis jump values as indicated on the hysteresis curve of Fig. 7(c) to jump between the hysteresis values of V_{dd} and V_{ss}.

In summary, the Schmitt trigger circuit of Fig. 7(a) gives the hysteresis needed for the generic multivibrator of Fig. 1(a), with the hysteresis parameters given in terms of the circuit parameters of Fig. 7 by

$$Y_{hi} = V_{dd}, \quad Y_{lo} = V_{ss}, \quad X_{lo} = \frac{V_{ss} + aV_{bias}}{1+a}, \quad X_{hi} = \frac{V_{dd} + aV_{bias}}{1+a} \tag{22}$$

Because we have four values (a, V_{bias}, V_{dd}, V_{ss}) to set the hysteresis and four circuit parameters available, we can obtain reasonable multivibrators using the circuits developed to this point.

It should be noted that transistorized versions of the Schmitt trigger exist and can be used in place of the op-amp circuit as shown in Fig. 7(a). See Ref. 2, p. 317 for a BJT-Resistor type Schmitt trigger and Ref. 2, p. 321 for a CMOS type. However, it is to be pointed out that these lack the sharpness and flexibility for design of the op-amp Schmitt trigger. An operational transconductance amplifier (OTA) version of the Schmitt trigger can be found in Ref. 7.

LOGIC GATE CIRCUITS

It is also possible to construct multivibrators using digital gates; in fact this is probably the most frequently used method. Most books on digital circuits cover these multivibrators (see, for example, Ref. 8 as well as Ref. 4). Using only two-input NOR gates, Fig. 8(a) shows a monostable, Fig. 8(b), an astable, and Fig. 8(c) a bistable multivibrator. Throughout Fig. 8 the NOR gates, with their inputs tied together, act as inverters, so that they can be replaced to advantage by inverters. Figure 8(c) is an SR (set-reset) flip-flop with its S and R inputs made complementary to force the bistable state determinations. Also, throughout Fig. 8, the NOR gates can be replaced by NAND gates and similar behavior obtained by using triggers inverse to those used for the NOR gates. Although the use of standard gates makes these gate-constructed multivibrators attractive, and they work at relatively high pulse rates, their characteristics are not as sharp as those obtained from the op-amp Schmitt trigger circuits.

An astable circuit often used for precision clocks and using crystal control is shown in Fig. 9 (6, p. 930), where the inverters again can be made with NOR or NAND gates. The inverter on the right of Fig. 9 is used to square up the signal generated by the crystal, which acts as a second-order system to produce sinusoidal oscillations. Setting $s = jw$ in the characteristic equation found from Kirchhoff's laws, we see that the inverter gains need to be set to -2 to force the real part of the characteristic equation to zero; this is done by the choice of equal resistors. From the imaginary part, the square of the radian frequency of oscillations of such an oscillator is $1/LC$, where L and C are the equivalent inductance and capacitance of the crystal; consequently the period of the output pulses is $2\pi\sqrt{LC}$. A commonly used inverter comes in a package of six and is known as the 74LS04 (9, p. 779).

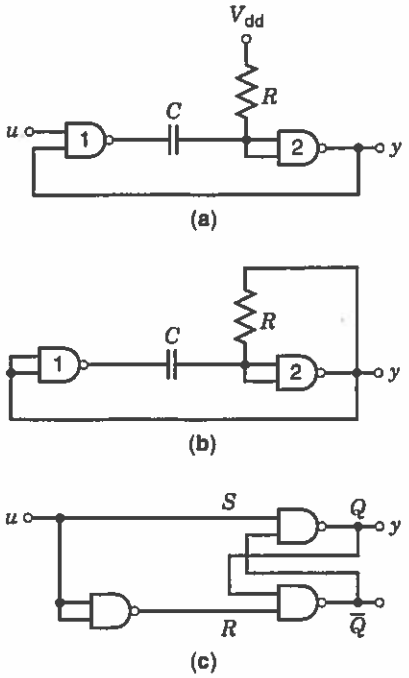

Figure 8. NAND realization of (a) monostable multivibrator, (b) astable multivibrator, and (c) bistable multivibrator.

THE 555 TIMER

A standard commercial package that can be used to make any of the multivibrators is the 555 timer, for which a full circuit

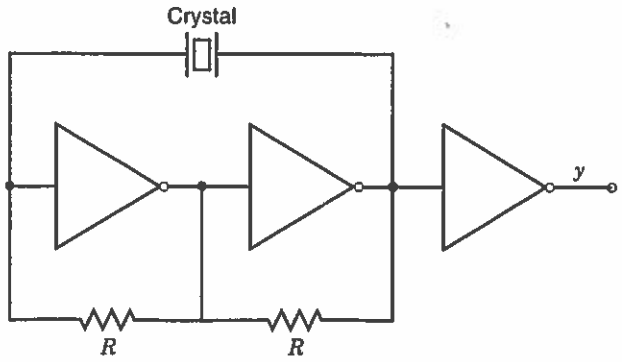

Figure 9. Astable multivibrator using crystal pulse repetition rate control and inverters.

diagram can be found in Ref. 10, pp. 9-33 through 9-38, along with settings and applications. This is useful for printed circuit board designs using standard components. Because of its common use, the 555 timer is treated in most standard electronic circuits textbooks, such as Ref. 4, pp. 975–979 and Ref. 11, pp. 683–688, 767. It comes in an eight-pin package (or as the 556 14-pin dual set), these pins being 1 = ground, 2 = trigger, 3 = output, 4 = reset, 5 = control voltage, 6 = threshold, 7 = discharge and 8 = V_{cc} bias. It can set the timing from microseconds to hours, and can source or sink up to 200 mA at the output. Depending upon the external circuitry used, the 555 can serve many functions, including that of a bistable, monostable, or astable multivibrator with an adjustable duty cycle. Basically, the 555 is a set-reset flip-flop (a bistable multivibrator) surrounded by circuitry in the package that allows it to take on various uses depending upon external circuitry. Its voltage at the output pin, Q of the SR flip-flop, is set (to V_{cc}) when the threshold pin voltage falls below $V_{cc}/3$ and is reset (to ground) when the threshold pin voltage rises above $2V_{cc}/3$. Thus, by simple control on the threshold pin, a bistable multivibrator results. By controlling the threshold voltage with the external circuitry one readily obtains other behavior. For example, Fig. 10 shows the connections for the 555 as an astable multivibrator. Here the capacitor C charges from $V_{cc}/3$ to $2V_{cc}/3$ through $R_{7-8} + R_{6-7}$, and discharges from $2V_{cc}/3$ to $V_{cc}/3$ through R_{6-7} at times independent of V_{cc}, given respectively by

$$t_{\text{charge}} = 0.693(R_{7-8} + R_{6-7})C \quad \text{(output ending high)} \tag{23}$$

$$t_{\text{discharge}} = 0.693R_{6-7}C \quad \text{(output ending low)} \tag{24}$$

for a period and frequency of

$$T_{\text{period}} = 0.693(R_{7-8} + 2R_{6-7})C, \quad f = \frac{1}{T_{\text{period}}} = \frac{1.44}{(R_{7-8} + 2R_{6-7})C} \tag{25}$$

and a duty cycle of

$$\text{Duty cycle} = \frac{R_{6-7}}{R_{7-8} + 2R_{6-7}} \tag{26}$$

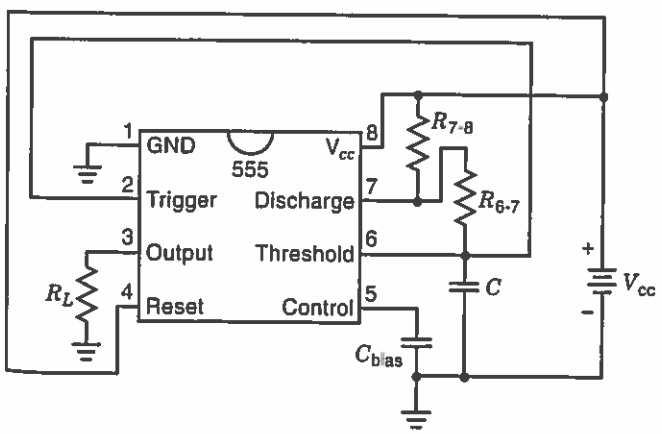

Figure 10. 555 Timer connected as an astable multivibrator.

Using these formulas with the three parameters available it is quite easy to design the 555 to give any reasonable duty cycle and oscillation frequency for a square wave going between ground (low) and V_{cc} (high). Data sheets show how to use it for such applications as frequency division, ramp generation, pulse width modulation, and pulse position modulation.

THE VAN DER POL OSCILLATOR

A robust astable multivibrator is obtained by using small damping in the van der Pol oscillator. The robustness results from the van der Pol oscillator being structurally stable, which makes it both practically and mathematically important. The van der Pol oscillator is described by the second-order differential equation

$$\frac{d^2y}{dt^2} + \epsilon(y^2 - 1)\frac{dy}{dt} + y = 0 \tag{27}$$

where ϵ is a parameter that determines the nature of the relaxation oscillation (ϵ small gives close to a sine wave, while ϵ large gives close to a square wave). Observing Eq. (27) we see that if $y^2 > 1$ then we have positive damping and the signal decays, while if $y^2 < 1$ there is negative damping and the signal grows; consequently the signal heads toward $y^2 = 1$. To set up a means to realize this multivibrator we first obtain the equivalent state variable description by rewriting Eq. (27) as

$$\frac{d^2y}{dt^2} + \frac{df(y)}{dy} + y = \frac{d\left(\frac{dy}{dt} + f(y)\right)}{dt} + y = 0 \tag{28}$$

$$f(y) = \epsilon\left(\frac{1}{3}y^3 - y\right) \tag{29}$$

Then by setting

$$x_1 = y \tag{30}$$

$$x_2 = \frac{dy}{dt} + f(y) = \frac{dx_1}{dt} + f(x_1) \tag{31}$$

and rewriting (30) and (31), upon using (28), we get

$$\frac{dx_1}{dt} = -f(x_1) + x_2 \tag{32}$$

$$\frac{dx_2}{dt} = -x_1 \tag{33}$$

Figure 11(a) shows a circuit realization of these equations using capacitors to form the derivatives, voltage-controlled current sources—made via transistors as differential pairs (12, p. 431) to realize the cross coupling, and a nonlinear (voltage-controlled) resistor to realize $f(\cdot)$. By changing the time scale and by multiplying the equations by constants, circuit components and waveform frequencies of interest can be obtained. However, this design is predicated on obtaining the cubic law nonlinear resistor, which is inconvenient. Fortunately, the equations are structurally stable and allow for similar results

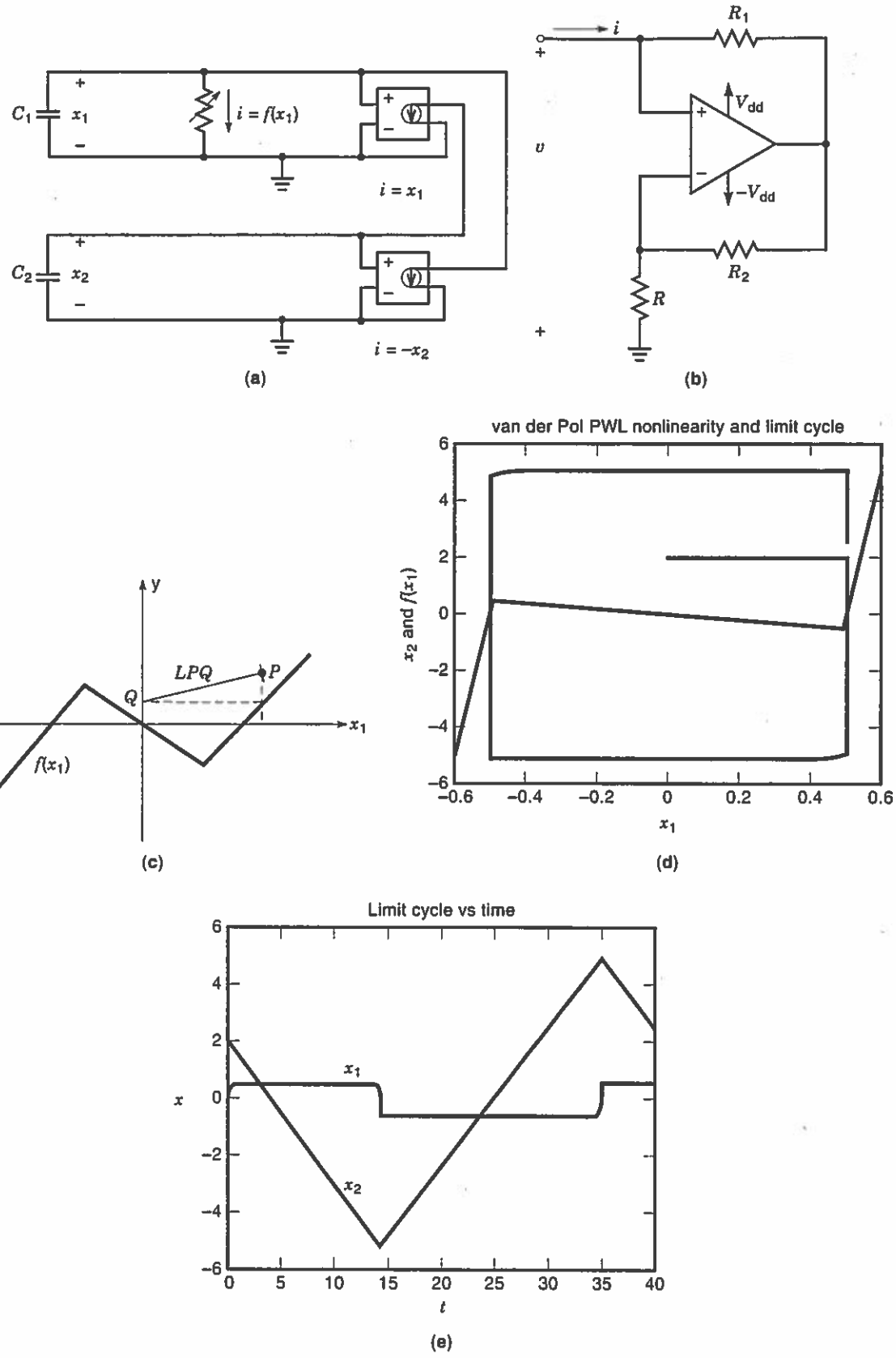

Figure 11. (a) A van der Pol oscillator constructed with voltage-controlled current. (b) Op-amp piecewise linear circuit to approximate cubic law of Eq. (29). (c) Limit cycle construction in state space. (d) Limit cycle obtained from Matlab runs of Eqs. (32) and (33) with piecewise linear $f(x_1)$. (e) Waveforms obtained from Matlab runs. $x_1(t)$ is a square wave and $x_2(t)$ is a triangular wave.

for a piecewise linear function approximation to the cubic. For this the cubic can be replaced by

$$f(x) = \begin{cases} ax - b & \text{for } x \le -d \\ -cx & \text{for } -d \le x \le d \\ ax + b & \text{for } d \le x \end{cases} \tag{34}$$

$$= ax - \frac{(a+c)}{2}\left|x + \frac{b}{a+c}\right| + \frac{(a+c)}{2}\left|x - \frac{b}{a+c}\right| \tag{35}$$

We can design this piecewise linear current vs voltage law, $i = f(v)$, via the op-amp circuit of Fig. 11(b), which results in the parameters

$$a = \frac{1}{R_1}, \quad b = \frac{V_{dd}}{R_1}, \quad c = \frac{R_2}{R_1 R}, \quad d = \frac{V_{dd}}{1 + \frac{R_2}{R}} \tag{36}$$

The van der Pol oscillator finally results by inserting the circuit of Fig. 11b into Fig. 11a.

To see the multivibrator nature of the van der Pol oscillator, we look at the limit cycle in state space. Figure 11(c) shows a plot of $f(x_1)$ inserted into the state space plane x_1–x_2. Trajectories in this state space are determined by Eqs. (32) and (33), for which we find, by simple division

$$\frac{dx_2}{dx_1} = \frac{-x_1}{x_2 - f(x_1)} \tag{37}$$

Consequently, the slope of the trajectory at any point is well determined, and we can construct the trajectory by determining this slope graphically as follows: Choose a point P of interest and drop a perpendicular to the x_1 and x_2 axes; that gives x_1 and x_2 at P, x_1P, and x_2P. Next drop a perpendicular from $f(x_1P)$ to the x_2 axis, intersecting at Q, and draw a line LPQ from P to Q. The slope of LPQ is $-1/(dx_1/dx_2)$ by (37), and by trigonometry the slope of the line perpendicular to LPQ is the negative inverse of this, which is dx_1/dx_2. Connecting nearby points on this line gives the trajectory. From this construction we can see that there is one limit cycle toward which all trajectories converge (except the [unstable] one at the origin). We also easily see that if the slope of the negative conductance portion is small in magnitude, then the limit cycle is close to a circle giving sinusoidal-like oscillations. But if the slope of the negative conductance portion of $f(\cdot)$ is large, then the oscillations are close to a square wave, as desired for a multivibrator. Figures 11(d)–(e) show a typical phase-plane plot of a limit cycle and waveforms obtained from Matlab runs.

By using an $f(v)$ which is odd, $f(v) = -f(-v)$, with multiple negative resistance regions, one can obtain many different limit cycles and consequently make a multivibrator that has more than two vibration levels.

TRANSISTORIZED CIRCUITS

Figures 12(a)–(b) show an astable BJT (Bipolar Junction Transistor) circuit (13, pp. 285–289) along with typical waveforms. Noting these waveforms, we see that transitions result at the end of the first-order exponential rises in the base-emitter voltages v_2 and v_3. If we take T_1 to be the time when v_1 is high, then $T_1 = R_3C_2 \ln 2$, which is found by equating

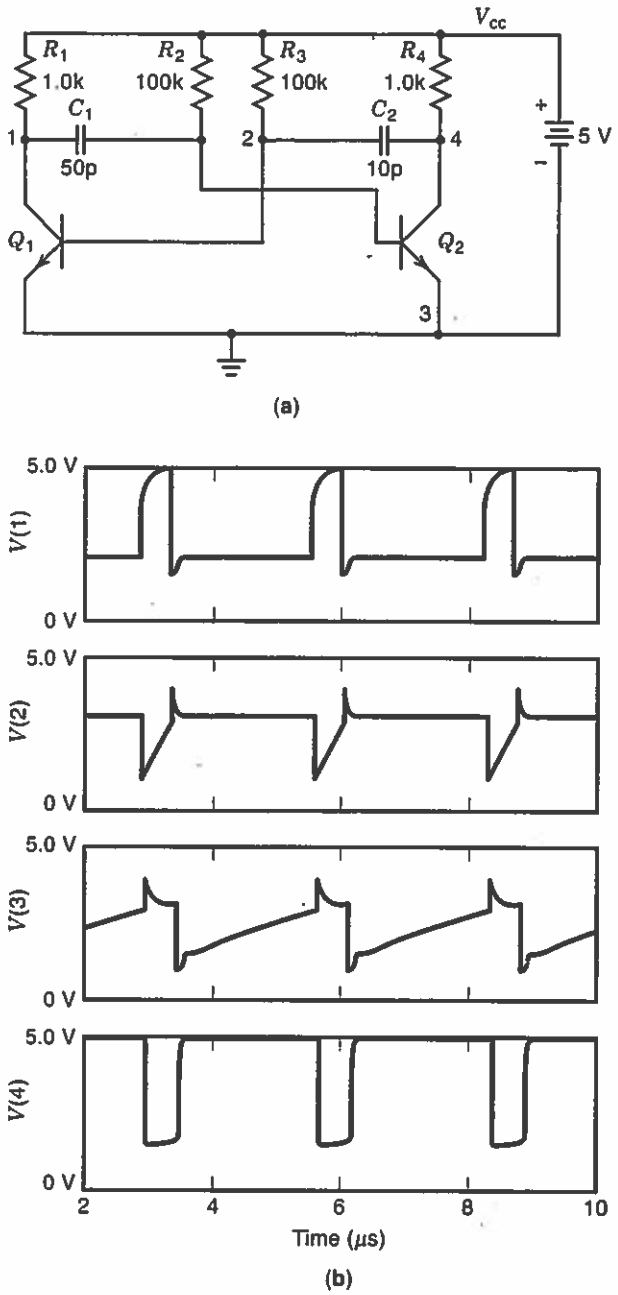

Figure 12. (a) BJT astable multivibrator. (b) Waveforms for the astable multivibrator obtained from PSpice runs.

the current in R_3 at T_1, of value $2V_{cc}/R_3$, to its exponentially decaying value from the previous transition, $(2V_{cc}/R_3)\exp(-T_1/(R_3C_2))$. For the value T_2 for which v_4 remains high, we similarly find $T_2 = R_2C_1 \ln 2$. Consequently, the period is independent of V_{cc} and is given by

$$T_{\text{period}} = T_1 + T_2 = 0.7(R_2C_1 + R_3C_2) \tag{38}$$

with various duty cycles possible.

Figures 13(a)–(b) show a bistable BJT multivibrator circuit (2, p. 300) with its node voltages. One of the two stable states is triggered by a positive pulse V_{in1}, of amplitude V_{cc}, at the left input, and the other by a similar pulse V_{in2} applied at

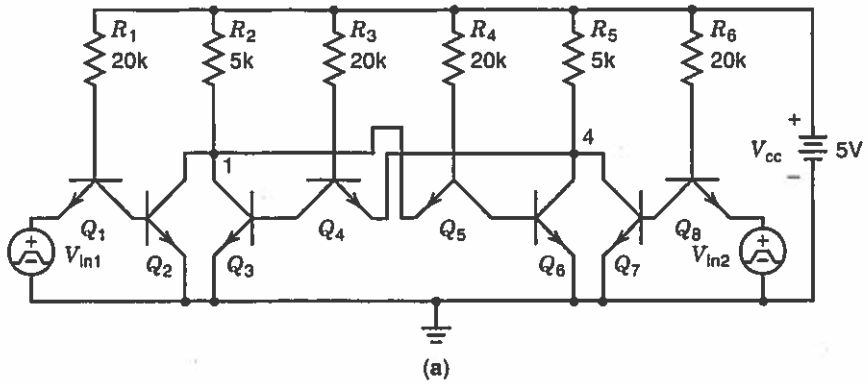

(a)

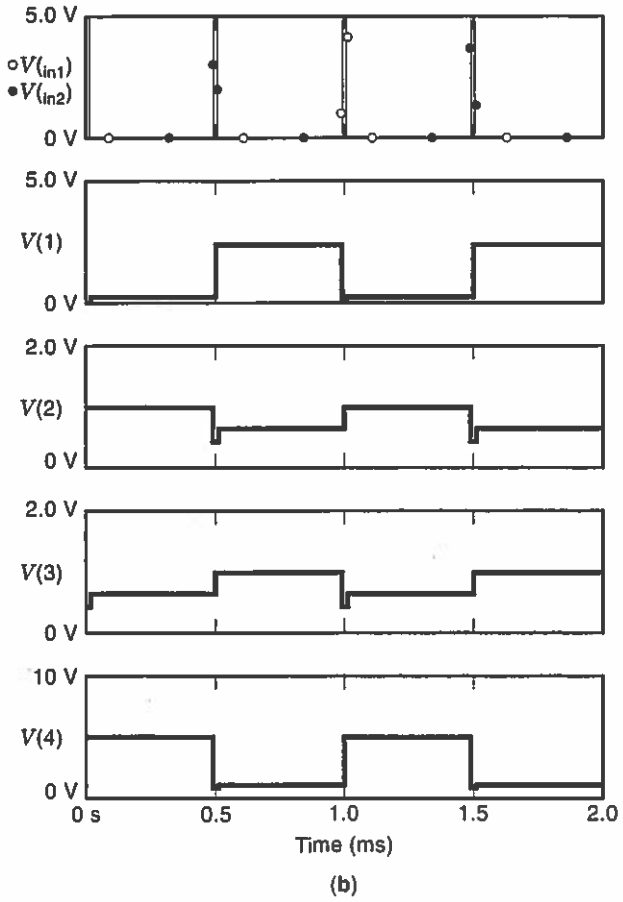

(b)

Figure 13. (a) BJT bistable multivibrator. (b) Voltage waveforms for the bistable multivibrator obtained from PSpice runs.

the right. As can be seen from the waveforms, a pulse at the right, on the emitter of Q_8, is transmitted through Q_8 to raise the base voltage of Q_7, which by its increased collector current causes v_4 to drop. In turn this drop is fed through Q_4, lowering the base-emitter voltage of Q_3 and decreasing the current in R_2 to raise v_1, which is fed back to the base of Q_6 via Q_5 to reinforce the lowering of v_4. The result of the positive feedback is a very sharp rise. Thus the risetime is limited only by the transition delays of the transistors.

Figures 14(a–b) show a BJT monostable multivibrator (13, pp. 290–292) along with typical waveforms. Essentially this is the multivibrator of Fig. 12(a), with C_2 replaced by a resistor and a voltage divider, including R_5 and V_{ss}, to insure that the base of Q_1 will be biased to bring the transition consistently to the same stable state. As can be verified from the waveforms, the pulse width is determined by the time constant that determines the rise of v_3. Since during the pulse transition, the transistor Q_1 (being saturated) acts as a short between collector and emitter, the time constant is just R_2C_1. Roughly, during the pulse, v_3 rises from $-V_{cc}$ to V_{cc} and stops when it reaches 0 (actually at V_{be}(on) of about 0.7 V). Because $v_3(t) = V_{cc} - 2V_{cc}\exp(-t/(R_2C_1)$ we calculate

$$T_{\text{pulse-width}} = R_2C_1 \ln 2 \tag{39}$$

The most frequent means of making multivibrators using MOS transistors are through the logic circuits shown in the logic gate circuits section above, where the gates are constructed in CMOS form, but others are described in the literature (14–16).

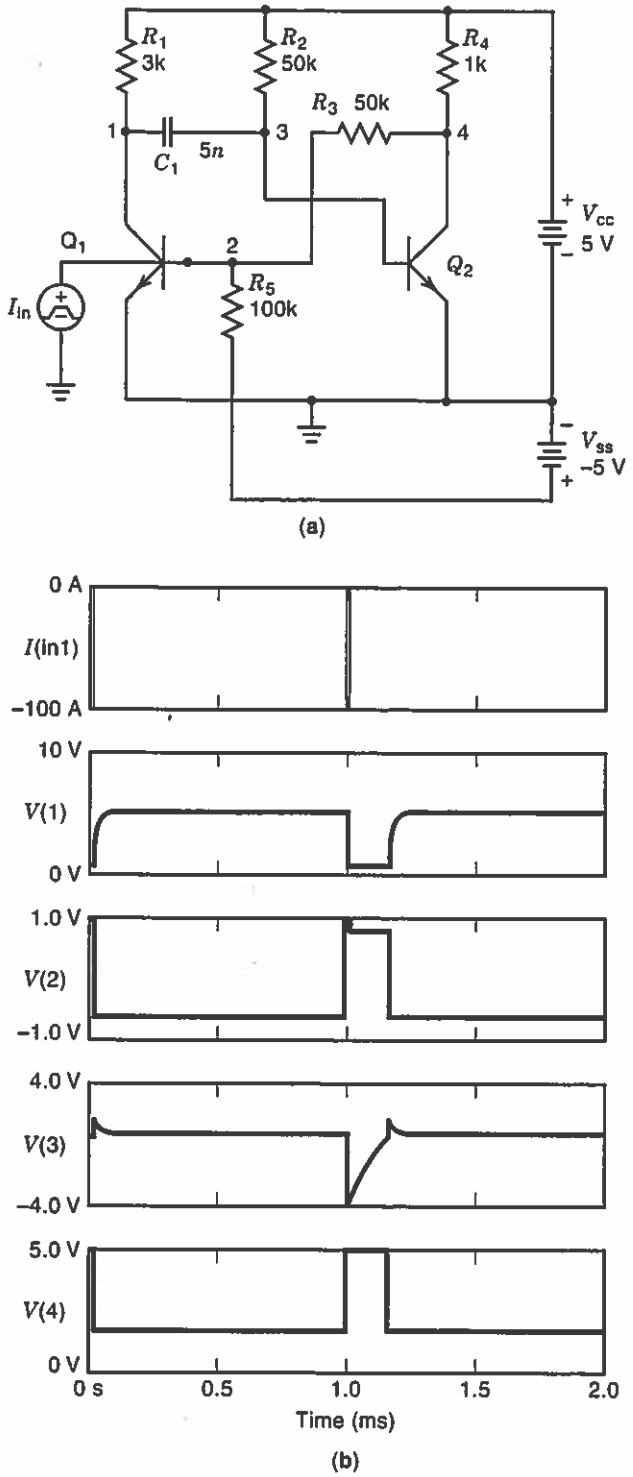

Figure 14. (a) BJT monostable multivibrator. (b) Voltage waveforms for the monostable multivibrator obtained from PSpice runs.

BIBLIOGRAPHY

1. A. S. Sedra and K. C. Smith, *Microelectronic Circuits*, New York: Oxford Univ. Press, 4th ed., 1997, Chap. 12.
2. D. A. Hodges and H. G. Jackson, *Analysis and Design of Digital Integrated Circuits*, 2nd ed., New York: McGraw-Hill, 1988, Chap. 8.
3. T. F. Schubert, Jr. and E. M. Kim, *Active and Non-Linear Electronics*, New York: Wiley, 1996, Chap. 13.
4. M. N. Horenstein, *Microelectronic Circuits and Devices*, 2nd ed., Upper Saddle River, NJ: Prentice-Hall, 1996, Sect. 15.2.
5. R. Boylestad and L. Nashelsky, *Electronics: A Survey*, 3rd ed., Englewood Cliffs, NJ: Prentice-Hall, 1989, Sect. 12.5.
6. S. D. Ferris, *Elements of Electronic Design*, Minneapolis, MN: West Publishing Company, 1995, Chap. 12.
7. B. Linaras-Barranco, E. Sanchez-Sinencio, and A. Rodriguez-Vazquez, CMDS circuit implementation for neuron models, *Proc. IEEE Int. Symp. Circuits Syst.*, New Orleans, LA, pp. 2421–2424, 1990.
8. J. M. Rabaey, *Digital Integrated Circuits*, Upper Saddle River, NJ: Prentice-Hall, 1996, Chap. 6.
9. A. J. Tocci, *Digital Systems, Principles and Applications*, 6th ed., Upper Saddle River, NJ: Prentice-Hall, 1995.
10. National Semiconductor, *Linear Databook*, Santa Clara, CA: 1982.
11. C. J. Savant, Jr., M. S. Roden, and G. L. Carpenter, *Electronic Circuit Design, An Engineering Approach*, Menlo Park, CA: Benjamin/Cummings, 1987.
12. R. L. Geiger, P. E. Allen, and N. R. Strader, *VLSI Design Techniques for Analog and Digital Circuits*, New York: McGraw-Hill, 1990.
13. P. H. Beards, *Analog and Digital Electronics*, 2nd ed., New York: Prentice-Hall, 1991.
14. I. M. Filanovsky and I. G. Finvers, A simple nonsaturated CMOS multivibrator, *IEEE J. Solid-State Circuits*, 23(1): 289–292, 1988.
15. D. J. Comer, *Electronic Design with Integrated Circuits*, Reading, MA: Addison-Wesley, 1981, Chap. 3.
16. G. M. Blair, Comments on new single-clock CMOS latches and flip-flops with improved speed and power savings, *IEEE J. Solid State Circuits*, 32(10): 1610–1611, 1997.

ROBERT W. NEWCOMB
University of Maryland, College Park

LOUIZA SELLAMI
U.S. Naval Academy

MULTIVIBRATORS. See VARIABLE-FREQUENCY OSCILLATORS.

MUSCLE SIGNALS. See ELECTROMYOGRAPHY.

MUSICAL INSTRUMENTS

An electronic musical instrument can be defined as an instrument in which sounds are produced through some form of electronic generation rather than through the acoustic resonance of a vibrating body. More succinctly, electronic instruments produce musical sound waves electrically rather than mechanically.

The introduction of electrically generated sounds, linked with the application of that technology into the production and design of musical instruments, created a revolutionary way of thinking about the very nature of musical instruments. Whereas traditional acoustic instruments relied upon mechanically vibrating bodies to generate sounds, electronic instruments rely upon the oscillation of an electrical current to simulate a musical wave form. Nearly all of the electronic

Wiley Encyclopedia of Electrical and Electronics Engineering

Volume 14

John G. Webster, Editor
Department of Electrical and Computer Engineering
University of Wisconsin–Madison

A Wiley-Interscience Publication
John Wiley & Sons, Inc.
New York · Chichester · Weinheim · Brisbane · Singapore · Toronto
1999